Prepared in collaboration with the U.S. Army Corps of Engineers

Barrier Island Habitat Map and Vegetation Survey—Dauphin Island, Alabama, 2015

Open-File Report 2017–1083

U.S. Department of the Interior
U.S. Geological Survey

Cover. Various habitats of Dauphin Island, Alabama.

Clockwise from top left: Beach habitat, beach habitat with intertidal flat, wooded dune habitat, intertidal marsh with black needlerush (*Juncus roemerianus*) and smooth cordgrass (*Spartina alterniflora*), slash pine (*Pinus elliotti*) forest habitat, black needlerush-dominated intertidal marsh, sea oats (*Uniola paniculata*), herbaceous dune, back-barrier shoreline with saltmeadow cordgrass (*Spartina patens*) and sea oats. Photographs by Michael J. Osland (U.S. Geological Survey, October 2015) and Sinéad M. Borchert (Borchert Consulting, October 2015).

Barrier Island Habitat Map and Vegetation Survey—Dauphin Island, Alabama, 2015

By Nicholas M. Enwright, Sinéad M. Borchert, Richard H. Day, Laura C. Feher, Michael J. Osland, Lei Wang, and Hongqing Wang

Prepared in collaboration with the U.S. Army Corps of Engineers

Open-File Report 2017–1083

U.S. Department of the Interior
U.S. Geological Survey

U.S. Department of the Interior
RYAN K. ZINKE, Secretary

U.S. Geological Survey
William H. Werkheiser, Acting Director

U.S. Geological Survey, Reston, Virginia: 2017

For more information on the USGS—the Federal source for science about the Earth, its natural and living resources, natural hazards, and the environment—visit https://www.usgs.gov or call 1–888–ASK–USGS.

For an overview of USGS information products, including maps, imagery, and publications, visit https://store.usgs.gov.

Suggested citation:
Enwright, N.M., Borchert, S.M., Day, R.H., Feher, L.C., Osland, M.J., Wang, Lei, and Wang, Hongqing, 2017, Barrier island habitat map and vegetation survey—Dauphin Island, Alabama, 2015: U.S. Geological Survey Open-File Report 2017–1083, 17 p., https://doi.org/10.3133/ofr20171083.

ISSN 2331-1258 (online)

Acknowledgments

This effort was one component of a larger effort funded by the National Fish and Wildlife Foundation (project ID: 45719) to investigate viable, sustainable restoration options that protect and restore the natural resources of Dauphin Island, Alabama. This effort was conducted in collaboration with the U.S. Army Corps of Engineers and in cooperation with the State of Alabama. We received assistance from numerous individuals with site accessibility for data collection. In particular, we thank Mayor Jeff Collier, Eliska Morgan, Justin McDonald, Elizabeth Godsey, the Bon Secour National Wildlife Refuge, the Dauphin Island Property Owners' Association, the Dauphin Island Audubon Bird Sanctuary, and William Dubose for their assistance. We also thank the Dauphin Island Sea Lab for accommodations during our field visits.

Contents

Figures

Tables

Conversion Factors

International System of Units to U.S. customary units

Multiply	By	To obtain
	Length	
centimeter (cm)	0.3937	inch (in.)
millimeter (mm)	0.03937	inch (in.)
meter (m)	3.281	foot (ft)
meter (m)	1.094	yard (yd)
kilometer (km)	0.6214	mile (mi)
	Area	
square meter (m^2)	10.76	square foot (ft^2)
square meter (m^2)	0.0002471	acre
square kilometer (km^2)	247.105	acre

Datum

Vertical coordinate information is referenced to the North American Vertical Datum of 1988 GEOID 12a (NAVD 88 Geoid 12a), unless otherwise noted.

Horizontal coordinate information is referenced to the North American Datum of 1983 Universal Transverse Meter Zone 16 North (NAD 83 UTM 16N).

Elevation, as used in this report, refers to distance above the vertical datum, unless otherwise noted.

Abbreviations

3DEP	3D Elevation Program (USGS)
ASPRS	American Society for Photogrammetry & Remote Sensing
CORS	Continuously operating reference station
DAS	Digital Aerial Solutions, LLC
DEM	Digital elevation model
DSM	Digital surface model
EHWS	Extreme high water springs
GNSS	Global Navigation Satellite System
lidar	Light detection and ranging
MMU	Minimum mapping unit
MSL	Mean sea level
NAVD 88	North American Vertical Datum of 1988

NDVI	Normalized difference vegetation index
NOAA	National Oceanic and Atmospheric Administration
PCA	Principal component analysis
RMSE	Root mean square error
RTK GPS	Real-time kinematic Global Positioning System
TPI	Topographic position index
USACE	U.S. Army Corps of Engineers
USGS	U.S. Geological Survey

Barrier Island Habitat Map and Vegetation Survey—Dauphin Island, Alabama, 2015

By Nicholas M. Enwright,[1] Sinéad M. Borchert,[2] Richard H. Day,[1] Laura C. Feher,[1] Michael J. Osland,[1] Lei Wang,[3] and Hongqing Wang[1]

Abstract

Barrier islands are dynamic environments due to their position at the land-sea interface. Storms, waves, tides, currents, and relative sea-level rise are powerful forces that shape barrier island geomorphology and habitats (for example, beach, dune, marsh, and forest). Hurricane Katrina in 2005 and the Deep Water Horizon oil spill in 2010 are two major events that have affected habitats and natural resources on Dauphin Island, Alabama. The latter event prompted a collaborative effort between the U.S. Geological Survey, the U.S. Army Corps of Engineers, and the State of Alabama funded by the National Fish and Wildlife Foundation to investigate viable, sustainable restoration options that protect and restore the natural resources of Dauphin Island, Alabama.

In order to understand the feasibility and sustainability of various restoration scenarios, it is important to understand current conditions on Dauphin Island. To further this understanding, a detailed 19-class habitat map for Dauphin Island was produced from 1-foot aerial infrared photography collected on December 4, 2015, and lidar data collected in January 2015. We also conducted a ground survey of habitat types, vegetation community structure, and elevations in November and December 2015. These products provide baseline data regarding the ecological and general geomorphological attributes of the area, which can be compared with observations from other dates for tracking changes over time.

Introduction

Barrier islands are coastal landforms consisting of wave-, wind-, and (or) tide-deposited sediments found along portions of coasts on nearly every continent (Oertel, 1985; Stutz and Pilkey, 2011). Like other coastal resources, barrier islands face an uncertain future heading into the latter part of the 21st century. Numerous threats, including hurricanes, accelerated sea-level rise, oil spills, and anthropogenic impacts, will influence the future of these islands (Pilkey and Cooper, 2014).

Barrier island systems provide numerous invaluable ecosystem services including storm protection and erosion control to the mainland, habitat for fish and wildlife, carbon sequestration in marsh habitats, water catchment and purification, recreation, and tourism (Barbier and others, 2011). The possible loss of these ecosystem services has prompted researchers to study the effects of accelerated sea-level rise on important barrier island habitats for resident and migratory shorebirds (Galbraith and others, 2014), neotropical migrants (Lester and others, 2016), and sea turtles (Katselidis and others, 2014).

Habitat mapping and vegetation surveys on barrier islands provide a valuable snapshot of the status of natural resources, and repeat assessments provide the ability to assess change over time (Kindinger and others, 2013). Highly accurate elevation data are critical for studying low-relief barrier island habitats. Elevation data are commonly combined with aerial photography for barrier island habitat mapping efforts (Chust and others, 2008; McCarthy and Halls, 2014; Zinnert and others, 2016). One challenge when using elevation data is related to a high degree of error in densely vegetated areas such as emergent wetlands. Studies have found that elevation data uncertainty in marsh can be as high as 60 centimeters (Medeiros and others, 2015; Buffington and others, 2016). Elevation uncertainty of digital elevation models (DEMs) is often not addressed, yet the level of uncertainty becomes critical when studying low-relief environments where centimeters can make a difference in estimating the exposure to physically demanding abiotic conditions. Monte Carlo simulations provide an efficient way to incorporate vertical uncertainty of a DEM through propagation of error and bias to produce probabilistic outputs (Hunter and Goodchild, 1995; Wechsler and Kroll, 2006; Cooper and Chen, 2013).

---

[1]U.S. Geological Survey.

[2]Borchert Consulting, Lafayette, LA, USA.

[3]Louisiana State University, Baton Rouge, LA, USA.

In this study, we produced a detailed map of barrier island habitats on Dauphin Island, Alabama, by using object-based image analyses (Blaschke and others, 2014), tide data, lidar data that incorporated elevation uncertainty by using Monte Carlo simulation to estimate probability surfaces for intertidal areas and areas above water levels during extreme storms, respectively, topography, surface elevation, 1-foot (ft) aerial imagery, and other ancillary data (for example, road data and salinity data; fig. 1). As part of this effort, we also conducted a survey of habitat types, vegetation community, and elevations from mid-November 2015 to mid-December 2015 along randomly placed transects at seven sites throughout the eastern half of the island (figs. 1 and 2). These products were developed as a component of a collaborative effort between the U.S. Geological Survey (USGS), the U.S. Army Corps of Engineers (USACE), and the State of Alabama funded by the National Fish and Wildlife Foundation to investigate viable, sustainable restoration options that protect and restore the natural resources of Dauphin Island, Alabama. The overarching goal of the aforementioned effort is to preserve and enhance the ecological functions and values of the island, including the adjacent estuarine and marine resources. The data collected during this study (Enwright and others, 2017) will help provide information on the current areal coverage and distribution of habitats and serve as a baseline for evaluating and predicting changes caused by gradual coastal processes, potential future episodic events, and potential restoration actions.

Dauphin Island

Dauphin Island, Alabama, is part of a 105-kilometer (km)-long wave-dominated Mississippi-Alabama barrier island chain. The island chain is backed by the shallow (less than 4 meters [m] deep) Mississippi Sound (Otvos and Carter, 2008). Dauphin Island is the only barrier island located offshore of coastal Alabama. Dauphin Island is about 25 km long and contains about 13.5 square kilometers (km^2) of emergent intertidal or supratidal habitats (fig. 2). Dauphin Island was formed about 3,500 to 5,000 years ago when the rising sea levels during the mid- to late Holocene Epoch led to the engulfment of a Pleistocene beach ridge (that is, a higher ridge on the eastern side of Dauphin Island) (Otvos and Carter, 2008). Barrier islands in the Mississippi Sound have experienced a strong westward movement due to longshore drift and westward littoral transport (Otvos, 1970; Morton, 2008).

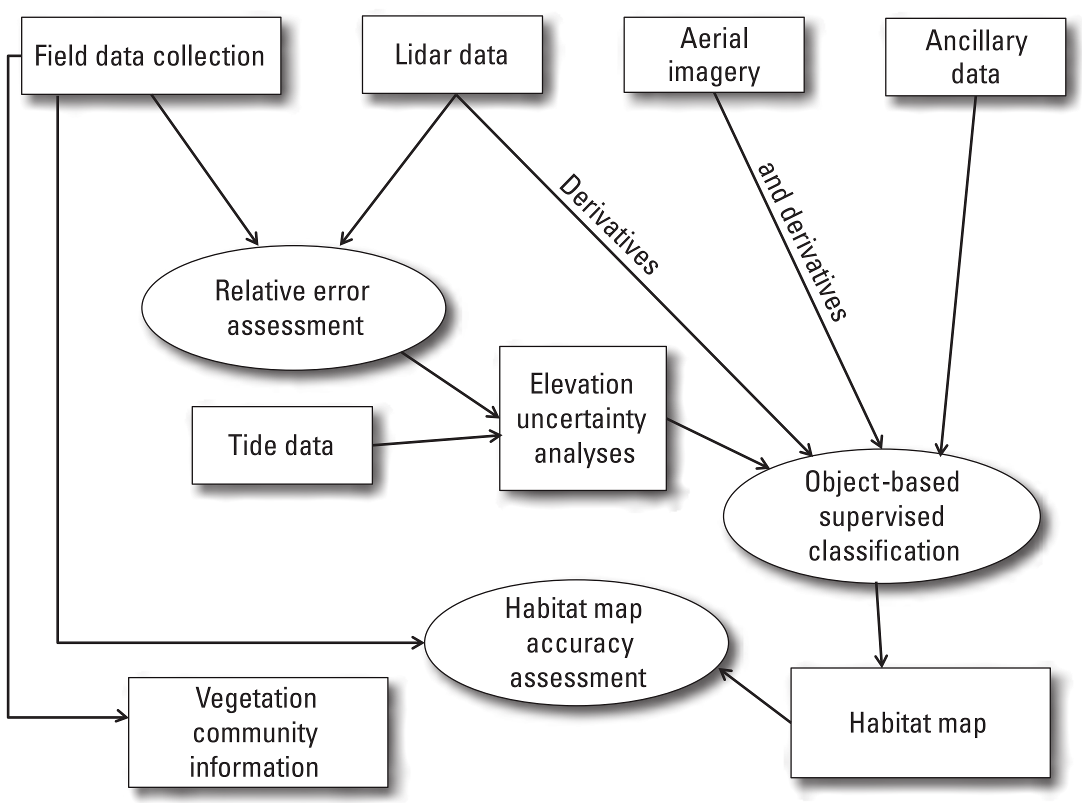

Figure 1. An overview of the development of a habitat map and collection of vegetation data, Dauphin Island, Alabama, 2015.

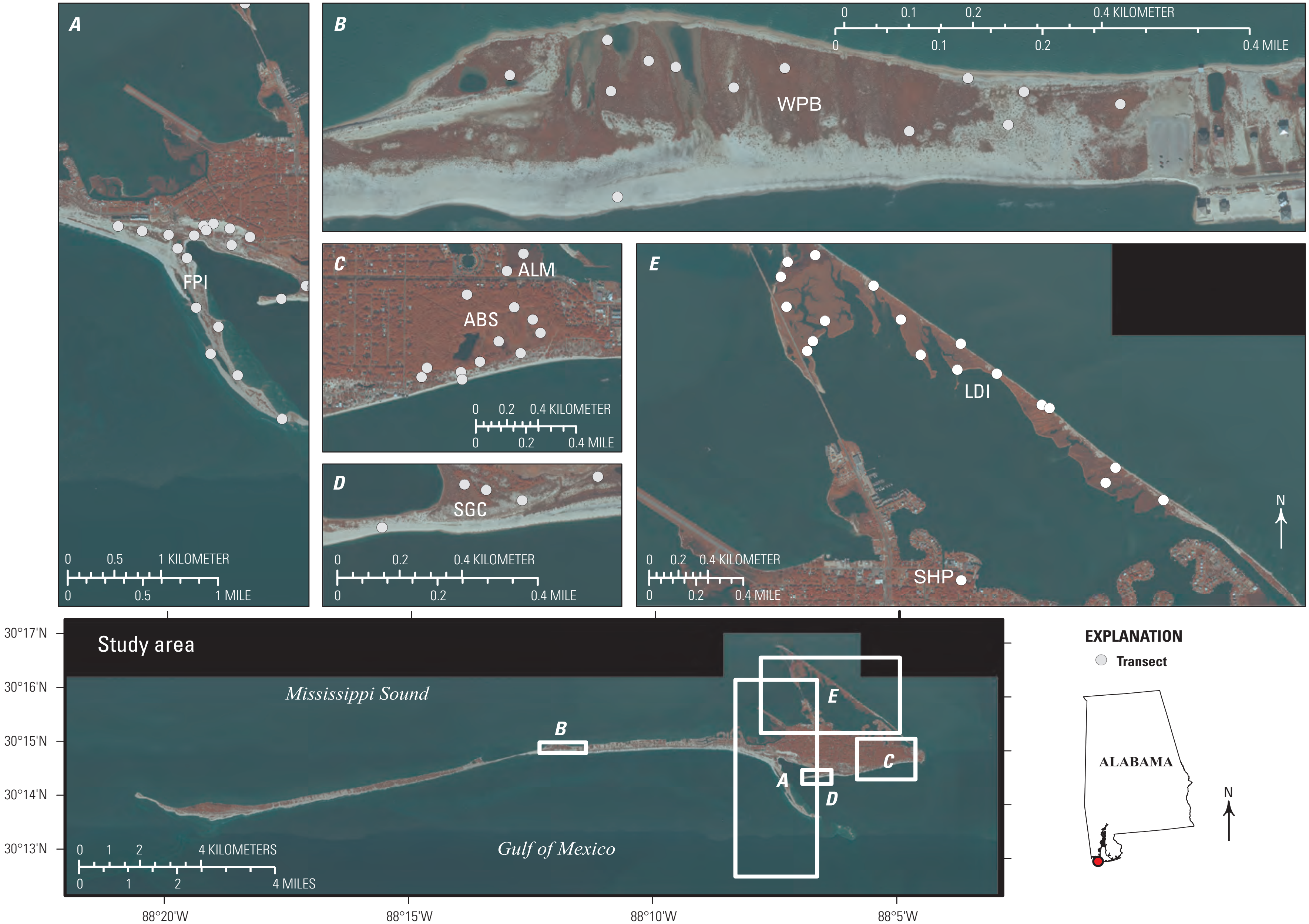

Bases from U.S. Geological Survey 1-ft aerial imagery, 2015,
Universal Transverse Mercator projection, Zone 16, NAD 83

Figure 2. Location of study area, sites, and transects, Dauphin Island, Alabama, 2015. [ABS, Audubon Bird Sanctuary site; ALM, State-owned marsh site; FPI, site near the Dauphin Island fishing pier; LDI, site on Little Dauphin Island; SGC, site south of the Isle Dauphine golf club; SHP, site at the Indian Shell Mound Park; WPB, site near West End Beach]

Methods

Field Data Collection

Field data were collected on Dauphin Island during two and a half weeks in November and December 2015. Vegetation and elevation data were collected by using cluster sampling at 67 different transects located across 7 different sites (fig. 2*A*–*E*). Other barrier islands in the Mississippi Sound are partially owned by the National Park Service; however, much of Dauphin Island is privately owned, including the entire western half of the island. Site selection was driven predominantly by accessibility. The transects, which covered 10 general habitat types, were randomly selected based on approximate coverage of general habitats per site from 1-m color-infrared aerial photography acquired in 2013 from the National Agriculture Imagery Program (table 1; U.S. Department of Agriculture, 2013).

Each transect consisted of three equally spaced plots. Transect lengths for nonforested and forested areas were 15 m and 30 m, respectively. For each transect, information was collected at a set of eight points radiating from the center point at a distance of about 25 m at intervals of 45-degree angles (fig. 3). Transects were oriented at an angle that would keep the specific transect within a single habitat. The location (that is, x,y coordinate and elevation relative to the North American Vertical Datum

Table 1. General habitat types at the centers of transects at sites on Dauphin Island, Alabama, 2015.

[See figure 2 for site locations]

Site[2]	Habitat at transect centers[1]										
	B	DB	DH	DW	F	IF	IM	M	SS	UBF	Total
ABS	0	0	0	3	4	0	0	2	1	1	11
ALM	0	0	0	0	1	0	1	0	0	0	2
FPI	2	1	4	2	1	0	0	5	0	2	17
LDI	0	0	0	0	1	3	6	4	3	1	18
SGC	0	0	1	0	0	0	0	1	2	1	5
SHP	0	0	0	0	1	0	0	0	0	0	1
WPB	1	0	0	0	0	1	6	4	0	1	13
Total	3	1	5	5	8	4	13	16	6	6	67

[1]B, beach; DB, dune, bare; DH, dune, herbaceous; DW, dune, wooded; F, forest, IF, intertidal flat; IM, intertidal marsh; M, meadow; SS, scrub/shrub; UBF, unvegetated barrier flat.

[2]ABS, Audubon Bird Sanctuary site; ALM, State-owned marsh site; FPI, site near the Dauphin Island fishing pier; LDI, site on Little Dauphin Island; SGC, site south of the Isle Dauphine golf club; SHP, site at the Indian Shell Mound Park; WPB, site near West End Beach.

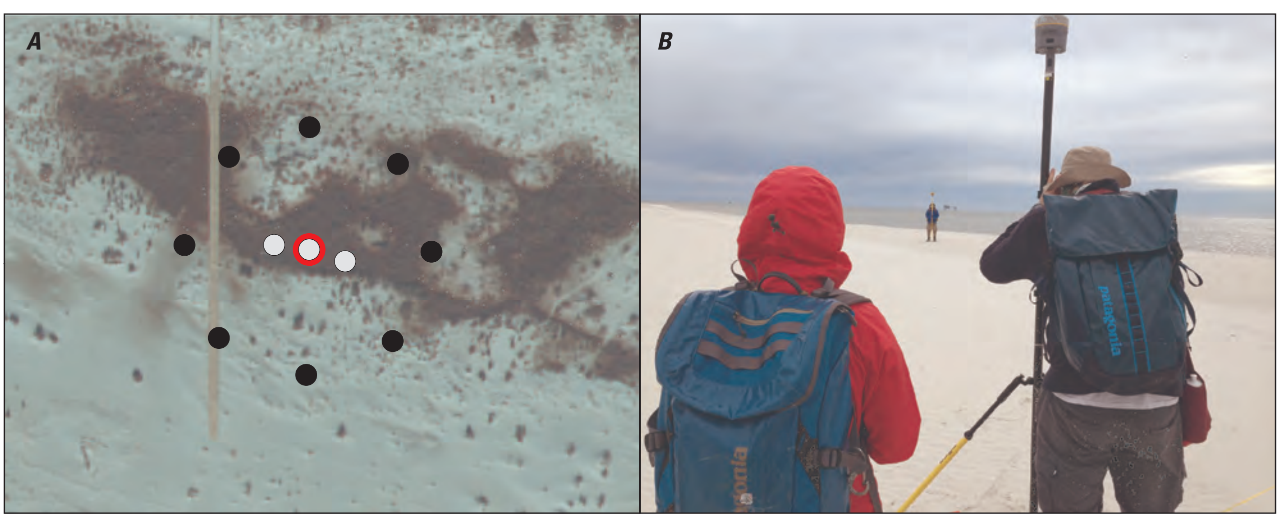

Figure 3. Overview of the field data sample design, Dauphin Island, Alabama, 2015. (*A*) A transect overlaid on 1-ft USGS aerial orthophotography from 2015. (*B*) Scientists measuring a radial offset point (the location in the background of the photograph) for beach habitat.

of 1988 [NAVD 88]) and habitat type were collected for all plots of a transect and radial points. A visual survey of vegetation cover by species was conducted for the three plots located along the transect (fig. 3). Vegetation cover data were collected within 1-square-meter (m^2) plots for vegetation heights below 1.4 m and above 1.4 m. For forest and scrub/shrub plots, canopy cover was surveyed for 100-m^2 plots. The dominant species per habitat were determined by using a vegetation importance value index (Curtis and McIntosh, 1951) modified via the omission of density (similar to Cole, 1978). This modification was necessary because species abundance, which would be required for the calculation of density, was not measured. Specifically, the dominant species per habitat were estimated by ranking the sum of the relative frequency and relative percent cover by habitat.

Elevation estimates were collected at the center point in the transect (gray point with a red halo in fig. 3*A*) by using a high-precision real-time kinematic (RTK) Global Positioning System (GPS) connected to a Global Navigation Satellite System (GNSS; Trimble R10 and TSC3, Trimble, Sunnyvale, Calif.), coupled with the continuously operating reference station (CORS) network for Mississippi and Alabama (University of Southern Mississippi's CORS network or the Alabama Department of Transportation's CORS). A laser rangefinder (Laser Technology, Inc., 360 R, Centennial, Colo.) was used to collect the position of the transect end points (gray points in fig. 3*A*) and the radial points by offsetting the RTK GPS point (black points in fig. 3*A*; fig. 3*B*). The elevation data collection process involved taking repeat observations at a specific point (n = 180) for which the precision was estimated for the set of observations for each RTK GPS point. SigmaPlot 12.5 (Systat Software, Inc., San Jose, Calif.) was used for all nonspatial statistical analyses in this study, unless otherwise noted. The distribution of precision estimates for all of the RTK GPS observations was right-skewed (that is, skewness = 1.09) with a median root mean square error (RMSE) of ±0.037 m.

Orthophotography and Lidar Elevation Data

Two main data sources for the habitat mapping effort included high-resolution orthophotography and lidar elevation data (fig. 1). We used project-specific 1-ft color-infrared aerial orthophotography acquired on December 4, 2015, by Digital Aerial Solutions, LLC (DAS; Riverview, Fla.) and the USGS. The imagery was collected with a Leica ADS100 (Sensor Head 100) digital camera (Wetzlar, Germany) when water levels were near or below mean sea level. All data for this study were in the Universal Transverse Mercator Zone 16 North projected coordinate system with the North American Datum of 1983.

We used topographic aerial lidar acquired during January 2015 by DAS and the USGS. The lidar data were collected by using the Leica ALS60 and ALS80 sensors. This data collection occurred over an extensive area (5,400 km^2) that included barrier islands in Alabama, Mississippi, and Terrebonne Basin, a large estuary in Louisiana. The data adhered to the USGS quality level 2 standards (Heidemann, 2014) and included the development of a 1-m DEM to support the USGS 3D Elevation Program (3DEP) (Sugarbaker and others, 2014). See Heidemann (2014) and Arundel and others (2015) for more information on USGS standards for lidar acquisition and 1-m DEM development. The vertical datum of the data was the NAVD 88 GEOID 12a. A vertical accuracy assessment was conducted by DAS for the 1-m DEM product based on standards outlined by the American Society for Photogrammetry and Remote Sensing (ASPRS, 2015). ASPRS (2015) recommends using the 95th percentile error for distributions for vegetated land covers instead of the estimates based off the RMSE. The assessment results indicated that the 95th percentile error for all habitat types was 0.305 m and 0.283 m for the lidar point cloud and the 1-m DEM, respectively. We also developed a 5-m DEM by resampling the 1-m DEM to a 5-m DEM by using bilinear interpolation.

Tide and Water Level Data

Vertical datum transformation involves transformation of a vertical datum from an orthometric datum (such as NAVD 88) to a locally relevant tidal datum. Data from the National Oceanic and Atmospheric Administration (NOAA) Dauphin Island tide gauge (station ID: 8735180) located on the eastern end of Dauphin Island were used for this study. For this gauge, the mean sea level (MSL) was estimated to be 0.018 m higher than NAVD 88 for the current National Tidal Datum Epoch. We transformed the vertical datum of the DEMs to MSL by adding this relative height difference to the DEM. Esri ArcMap 10.4.1 (Redlands, CA) was used for all spatial analyses, unless otherwise noted.

Two specific subobjectives of this effort were to (1) identify tidal water levels that could be used to map the intertidal ecotone, and (2) identify elevations that would likely be affected by extreme events. Cowardin and others (1979) define intertidal wetlands as those wetlands that fall above the extreme low water springs and below the extreme high water springs (EHWS) tidal datums. We defined EHWS as the highest astronomical tide (0.448 m relative to MSL), which is the highest predicted water level under astronomical conditions alone. Because airborne topographic lidar data did not include bathymetric data, our analyses were limited to the intertidal zone above MSL. We obtained the elevation for an extreme water level with a 10-percent annual exceedance probability from the NOAA Extreme Water Analyses for Dauphin Island based on observations between 1966 and 2010 (Zervas, 2013). We used the updated estimate for 2016 (1.13 m relative to MSL) which accounts for the relative sea-level-rise trend observed at the Dauphin Island gauge (NOAA, 2013).

Habitat Types

A custom 19-class habitat classification scheme was developed for this study through the review of various other barrier island mapping efforts. Note that the habitat classes (table 2) and habitat types noted in the field (table 1) do not have a one-to-one relationship. As work began on the habitat mapping effort, some habitat definitions were broadened; for example, slack and wet meadow were grouped into a single meadow class. In some cases, classes were expanded to add detail. For example, the dune class was split into three classes: (1) dune, bare, (2) dune, herbaceous, and (3) dune, wooded. These modifications were made to increase mapping feasibility and to ensure that mapped habitats met larger project needs (for example, linking barrier island habitats to faunal species).

Table 2. Habitat classes, description, description source, and reference points on Dauphin Island, Alabama, 2015.

[ppt, parts per thousand; m, meter]

Habitat	Description[1]	Source	Reference points[2]
Dune, bare	Dunes are supratidal features developed via Aeolian processes. Dunes are often found above water levels during storms and have a well-defined relative elevation (that is, upper slope or ridge). Dune, bare includes dunes that have less than 10 percent vegetation cover.	Acosta and others, 2005	21 (9)
Dune, herbaceous	Dune, herbaceous includes low-elevation dunes with sparse to dense herbaceous vegetation coverage. Herbaceous vegetation cover should generally be greater than or equal to about 10 percent. See the Dune, bare class for a general description of dune features.	Gibson and Looney, 1992	78
Dune, wooded	Dune, woody includes relatively immobile secondary dunes that support sparse vegetation coverage by shrubs. Compared to the other dune classes, these dunes are typically found at higher elevations and further from the shoreline. Woody vegetation cover should generally be greater than or equal to about 30 percent. See the Dune, bare class for a general description of dune features.	Lucas and Carter, 2010	36
Meadow	Meadow includes areas with sparse to dense herbaceous vegetation located above extreme high water springs found leading up to primary dunes and on the barrier flat (that is, backslope of dunes). Vegetation coverage should be generally greater than 30 percent.	Lucas and Carter, 2010	173
Unvegetated barrier flat	Unvegetated barrier flat includes flat or gently sloping unvegetated or sparsely vegetated areas (that is, less than 30 percent cover) above extreme high water springs that are located on the backslope of dunes, unvegetated washover fans, unvegetated open developed areas, and estuarine shorelines where salinity is less than 30 ppt.	Leatherman, 1979	40
Scrub/shrub	Scrub/shrub includes areas where woody vegetation height is greater than about 0.5 m, but less than 6 m. Woody vegetation coverage should generally be greater than 30 percent.	Cowardin and others, 1979	69
Forest	Forest includes upland areas where woody vegetation height is greater than 6 m. Woody vegetation coverage is generally greater than 30 percent.	Cowardin and others, 1979	87
Forested wetland	Forested wetland includes all nontidal wetlands dominated by woody vegetation with a height greater than or equal to 6 m. Woody vegetation coverage should generally be greater than 30 percent.	Cowardin and others, 1979	0
Intertidal beach	Intertidal beach includes bare or sparsely vegetated areas along the ocean-facing side of the island found between extreme low water springs and extreme high water springs that are adjacent to high-energy shorelines which occasionally experience salinity that is greater than or equal to 30 ppt.	Cowardin and others, 1979	5 (25)
Beach	Beach includes bare or sparsely vegetated area that is upslope of the intertidal beach zone and marine open water. These habitats occasionally experience inundation by marine water at a concentration of greater than or equal to 30 ppt and also include shorelines with high wave energy.	Cowardin and others, 1979	29 (1)

Table 2. Habitat classes, description, description source, and reference points on Dauphin Island, Alabama, 2015.—Continued

[ppt, parts per thousand; m, meter]

Habitat	Description[1]	Source	Reference points[2]
Intertidal flat	Intertidal flat includes all tidal wetlands (that is, wetlands found above extreme low water springs and below extreme high water springs) adjacent to estuarine open water (that is, water with salinity due to ocean-derived salts that would rarely be above 30 ppt) and along shorelines with low wave energy with vegetation cover of less than 30 percent.	Cowardin and others, 1979	66
Intertidal marsh	Intertidal marsh includes all tidal wetlands (that is, wetlands that are found above extreme low water springs and below extreme high water springs) with 30 percent or greater areal cover by erect, rooted, herbaceous hydrophytes.	Cowardin and others, 1979	145
Seagrass	Seagrass includes any combination of patchy or continuous submerged vegetation (that is, seagrasses, oligohaline grasses, attached macroalgae, and drift macroalgae) that covers 10 to 100 percent of the substrate. Areas mapped as seagrass were predominately obtained from 2015 generalized seagrass maps developed by Barry Vittor and Associates, Inc.	Finkbeiner and others, 2001	0
Oyster reef	Oyster reef includes subtidal and intertidal estuarine areas that are dominated by ridge-like or mound-like structures formed by the colonization and growth of extensive exoskeleton-building sessile invertebrates. Areas mapped as oyster reef were obtained from 1968 survey data (May, 1971) and oyster leases obtained from the State of Alabama.	Cowardin and others, 1979	0
Shoreline protection	Shoreline protection includes areas that have any material used to protect shorelines from erosion.	Fearnley and others, 2009	0
Developed	Developed includes areas dominated by constructed materials (that is, transportation infrastructure, and residential and commercial areas).	Homer and others, 2015	0
Open water, fresh	Open water, fresh includes all areas of nontidal open water (that is, isolated low-lying areas that are not influenced from tides associated with extreme high water spring tides). These open water areas generally have less than 30 percent cover of vegetation.	Cowardin and others, 1979	0
Open water, estuarine	Open water, estuarine includes all areas of tidal open water and estuarine water of the back-barrier side of the island (that is, water bodies that receive regular inundation from tides). These areas rarely have salinity greater than 30 ppt. These open water areas generally have less than 30 percent cover of vegetation.	Cowardin and others, 1979	0
Open water, marine	Open water, marine includes all areas of marine open water found offshore of the ocean-facing side of the island. These areas are found along high-energy coastlines and (or) occasionally experience salinity levels greater than or equal to 30 ppt.	Cowardin and others, 1979	0

[1]All percent coverage requirements refer to an area of at least 40 square meters (that is, the same area as the minimum mapping unit).

[2]Supplemental reference points are enclosed in parentheses. These points were created by using photointerpretation and analysis of elevation data.

DEM Error and Bias

The propagation of lidar data vertical uncertainty by using a Monte Carlo simulation requires an estimate of lidar DEM error and bias. We developed two different relative vertical error and bias estimates by comparing elevation collected via RTK GPS with the 1-m DEM. We used RTK GPS precision analyses and assumed that points that were within ±0.04 m were not different for determining the percentage of observations that were biased high (that is, the DEM is higher than RTK GPS observation).

The first estimate was developed from field data collected during this study for intertidal and wetland areas, collectively. Here, we used 62 RTK GPS points collected in intertidal flat (n = 7), intertidal marsh (n = 29), and meadow (n = 26) habitats, respectively. The rationale for inclusion of meadow was that these areas tend to have similar vegetation, such as *Spartina patens* and *Fimbristylis spadicea*, or vegetation structure as some intertidal marsh areas. These points generally represent low-lying areas. The sample had a median elevation of 0.405 m (relative to NAVD 88) and an interquartile range of 0.476 m. The sample was right-skewed (skewness = 0.545) with a bias high of 76 percent and a 95th percentile error of 0.415 m (table 3). The second estimate was developed from field data collected for dunes below 3 m relative to NAVD 88. The dune sample (n = 29) had a median elevation of 1.422 m (relative to NAVD 88) and an interquartile range of 1.522 m. These data were left-skewed (skewness = –2.583) with a bias high of 55 percent and a 95th percentile error of 0.160 m (table 3).

Monte Carlo DEM Error Propagation

Monte Carlo simulations provide an efficient way to propagate vertical error into DEMs for coastal applications involving tidal datums and sea-level rise (Cooper and Chen, 2013). In this study, error propagation followed an approach similar to that of Cooper and Chen (2013), with the addition of enhancements such as a neighborhood spatial autocorrelation filter and bias constraint used by Wechsler and Kroll (2006).

Figure 4 shows a general overview of the Monte Carlo simulation process. The first step in the error propagation is the development of a random field (that is, a raster with a normal distribution with a mean of 0 and a standard deviation of 0.5). We forced the bias to be either high or low for each random field, collectively based on the proportional bias high identified in the relative elevation analyses (table 3). Next, a local filter (a 3-by-3-pixel neighborhood) was used to incorporate spatial autocorrelation into the simulated random fields (Wechsler and Kroll, 2006). The filtered raster was multiplied by the 95th percentile error and added to the original DEM (table 3). Pixels were coded as a binary variable as being true (“1”) or false (“0”) given a specific condition relative to an elevation threshold (that is, less than or equal to EHWS and greater than or equal to the water level during an extreme storm, respectively). These binary rasters were summed, and the probability was determined by dividing by the iteration count (n = 1,000). A Monte Carlo simulation was run to estimate the probability of a pixel being less than or equal to EHWS and the probability of a pixel being greater than or equal to the water level during an extreme storm by using the respective error and bias estimates found in table 3. The Monte Carlo simulation associated with EHWS used the error and bias associated with intertidal areas and wetlands, and the Monte Carlo simulation associated with water levels during a storm used the dune error and bias. A python script was developed to implement the previous steps in Esri ArcMap 10.4.1.

Habitat Mapping

We used a semi-automated approach to classify barrier island habitats. A few preprocessing steps included conducting a principal component analysis (PCA) of the four-band aerial imagery and developing a normalized difference vegetation index (NDVI). We used multiresolution segmentation (Trimble, 2016) in Trimble eCognition Developer 9.2 (Munich, Germany) to segment imagery into objects based on spatial and spectral similarities with regards to derivatives of aerial imagery including the first two PCA components, NDVI, and elevation. We determined the optimal segmentation parameters (that is, bands, weights, and scale of objects) by using a trial-and-error approach, similar to other studies (Myint and others, 2006).

Table 3. Error and bias from relative vertical accuracy assessments of field data from the Dauphin Island study area, Alabama, 2015.

[%, percent; n, number; m, meter]

Measure	Intertidal and wetland	Dune
Bias high	Unvegetated: 57.1% (n = 7) Vegetated: 94.5% (n = 55) Average: $\bar{X}$ = 76% (n = 62)	Average: $\bar{X}$ = 55% (n = 29)
Skewness	0.545	–2.583
95th percentile error (m)	0.415	0.160

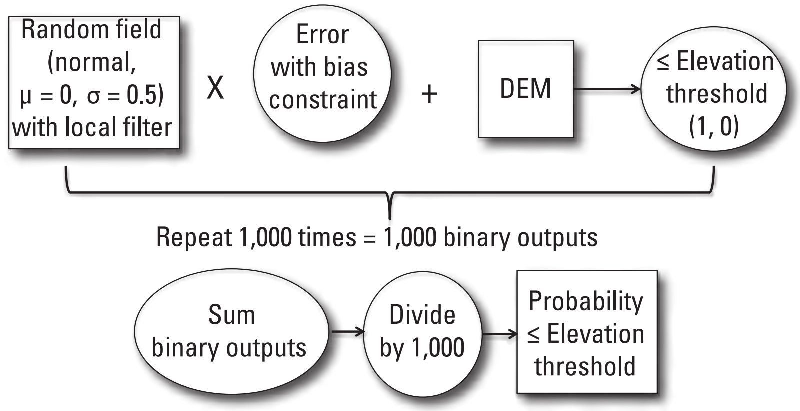

Figure 4. An overview of the Monte Carlo error propagation process for estimating the probability of a pixel being below or equal to the elevation of extreme high water springs (EHWS), Dauphin Island, Alabama. A similar process was used to estimate the probability of a pixel being greater than or equal to an extreme water level with a 10-percent annual exceedance probability. [DEM, digital elevation model]

We used a hierarchical approach to classify the image segments based on object-level statistics (for example, mean, standard deviation, and minimum; fig. 5). First, we classified the image segments as either land or water. Next, we classified land segments into vegetated and unvegetated categories by using trial and error with level-slice thresholds for NDVI and near-infrared spectral information. We used general knowledge-based thresholds to further subdivide vegetated and unvegetated areas into detailed barrier island habitats according to habitat definitions (table 2). For a given step, threshold-based rules were used to maximize omission errors while minimizing commission errors through visual inspection of results. After applying general decision rules for each habitat in a step-wise fashion, photointerpretation was conducted to refine habitats through manual editing.

Several elevation derivatives were developed to assist with habitat mapping of various classes including intertidal habitats, developed areas, scrub/shrub and forested habitats, and dune habitats. The Monte Carlo simulation previously discussed yielded the probability of a cell being below the EHWS, but did not explicitly consider connectivity. To incorporate connectivity, we removed low-elevation cells (that is, below the elevation of EHWS) that were not hydrologically connected to intertidal areas by removing isolated cells that lacked neighboring cells with a probability greater than 0.5 of being below elevations that could be intertidal (that is, we used an 8-side rule which includes cardinal and diagonal directions) (Poulter and Halpin, 2008). The resulting dataset was used as a guide for mapping intertidal habitats.

A digital surface model (DSM) can be helpful for estimating the height and morphology of building footprints (Meng and others, 2009) and the height of vegetation (Hudak and others, 2009). We used first returns from the lidar point cloud to create 1-m and 5-m DSMs by using the maximum bin algorithm (that is, assigning the DSM cell to be equal to the maximum first return in the cell). This relative difference between the DSM and the DEM (for example, the difference in the heights of objects such as tree canopy or buildings) was used to map developed areas (that is, building footprints) along with scrub/shrub and forested habitats.

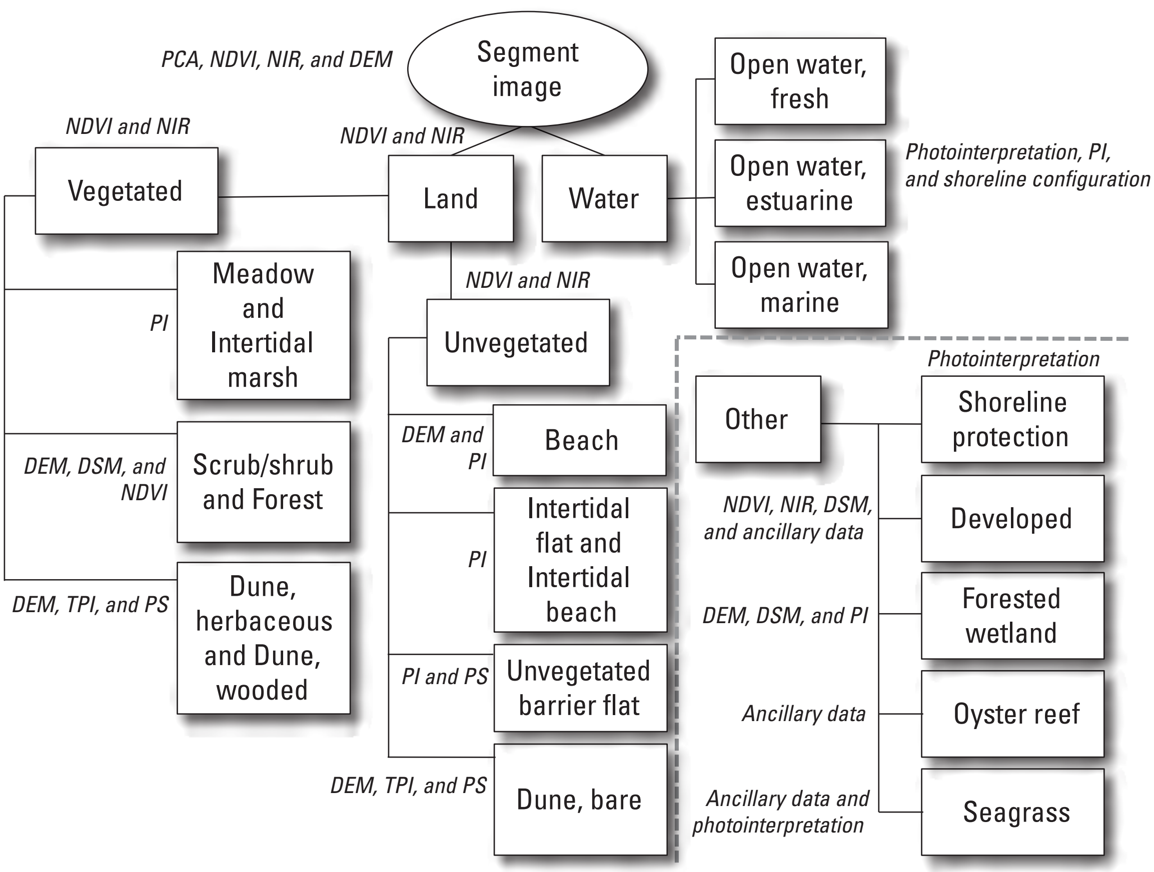

Figure 5. An overview of the habitat mapping process, Dauphin Island, Alabama. [DEM, digital elevation model; DSM, digital surface model; NDVI, normalized difference vegetation index; NIR, near-infrared band; PCA, principal component analysis; PI, probability of being intertidal; PS, probability of being above water levels during extreme storms; TPI, topographic position index; italics indicate data or techniques used for classifying each habitat]

We used a similar approach as Wernette and others (2016) to help guide dune delineation by using relative relief. The topographic position index (TPI) is developed by comparing the elevation for a pixel with the mean for the neighborhood (Weiss, 2001; De Reu and others, 2013). We estimated the TPI for a circular 30-m neighborhood. The optimal neighborhood size was determined through trial and error and visual interpretation. For the land portion of Dauphin Island, the mean and standard deviation of the relative difference between the center pixel and the mean neighborhood value were used to identify upper slopes and ridges. Upper slopes have a value between one-half and one standard deviation, and ridges have a value that is greater than one standard deviation from the regional mean (Weiss, 2001; De Reu and others, 2013). In addition to information on relative relief, we also used the probability raster for pixels being above the extreme water level with a 10-percent annual exceedance probability for delineating dunes.

We used secondary data for classifying oyster reef and seagrass habitats and refining developed areas. The oyster reef data represented historical oyster resources from 1968 survey data (May, 1971) obtained from the Alabama Department of Conservation and Natural Resources. Also, the oyster reef map contains locations of current oyster leases maintained by the State of Alabama. Seagrass data primarily came from an unpublished map developed by Barry Vittor and Associates, Inc., from aerial imagery from the fall of 2015, but also included some small areas evident in the December 2015 imagery, which is the source data mapped for this effort. To better capture transportation infrastructure, especially in areas where developed areas were obscured by tall tree canopy and tree shadow, we buffered road data from StreetMap North America (Esri ArcMap 10.4.1) by 2.5 m and classified areas falling within these buffers as developed. Salinity climatology data with a spatial resolution of 0.1 degree (about 11.12 km at equator) for the Gulf of Mexico were used to assist with interpretation of some habitat classes (table 2; Boyer and others, 2011).

Several post-processing steps were conducted to refine the barrier island habitat map while also reducing noise in the map. These steps included converting the image objects to a 1-m raster, applying a majority filter for a 3-by-3-pixel neighborhood, and applying a 40-square-meter (m^2) minimum mapping unit (MMU) to reduce noise. We selected this MMU as a reasonable balance between noise reduction and loss of detail evaluated through visual inspection. This mapping unit is well below the smallest minimum mapping unit (2,500 m^2) suggested by the USGS and the National Park Service for mapping vegetation in national parks (Lea and Curtis, 2010). Lastly, the map was reviewed for errors and manually edited as needed.

We conducted an accuracy assessment using field data, adhering generally to guidelines by Congalton and Green (2009). Instead of assessing map accuracy with points, we buffered field data to have area equal to the size of the MMU. As previously mentioned, the classes for the habitat map differed from the data collected in the field earlier in the project. Thus, we assessed and revised, as needed, the reference observations based on source data and derivatives used in this study (table 2). In order to have at least 30 accuracy points per class, supplemental data were added for the dune, bare; intertidal beach; and beach habitat classes. These supplemental points were attributed by using photointerpretation of source data and elevation derivatives. Elevation and relative topography information served as the critical factor in the determination of the habitat class for any supplemental data point. The accuracy for habitats with no ground reference points was not assessed. The accuracy assessment included overall accuracy, Kappa statistic (Cohen, 1960), and producer's and user's accuracy estimates for each class.

Results

The habitat map produced in this study is shown in figures 6 and 7. Of the nonwater, nondeveloped, subaerial habitats, the most abundant habitats were meadow (3.60 km^2, 29.2 percent), forest (2.92 km^2, 23.7 percent), intertidal marsh (1.22 km^2, 9.9 percent), dune, herbaceous (1.09 km^2, 8.8 percent), and unvegetated barrier flat (1.05 km^2, 8.5 percent; table 4). Collectively, these habitats account for about 80 percent of the nonwater, nondeveloped, subaerial habitat coverage. The map had an overall accuracy of 75.26 percent and a Kappa statistic of 0.72 (table 5). The dune, herbaceous class had the lowest producer's accuracy of just over 46 percent. In this instance, the majority of the omission errors were classified as meadow. This error is largely caused by the inability to identify small, relatively undefined dunes in the field that often lack defined relative topography, thus making them difficult to distinguish with repeatable methods by using remotely sensed data.

In addition to identifying the dominant types of vegetation for habitat classes (table 4), the vegetation survey provides information related to vegetation community at specific locations and general vegetation community estimates (that is, general percent coverage of any vegetation and vegetation height). The median total vegetation cover was 48 percent for all plots (n = 201). For nonforested and scrub/shrub plots (n = 162), the median total vegetation cover was 35 percent. About 75 percent of all plots had total vegetation cover greater than 10 percent. Beach and intertidal flat habitat classes (n = 42, collectively) had the sparsest cover. Only 11 percent of these plots were vegetated, and the median total vegetative cover was only 1 percent.

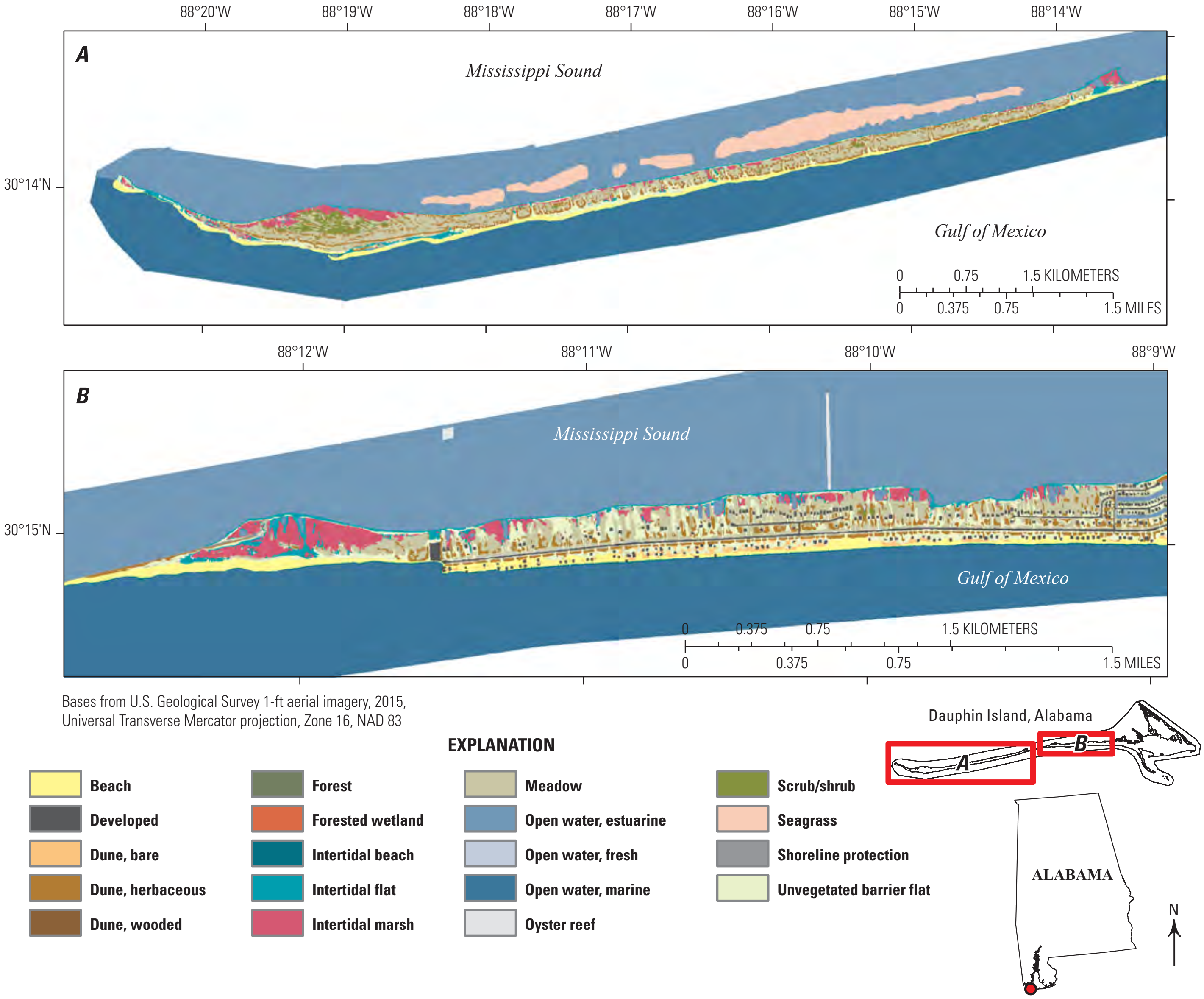

Figure 6. Habitat map for the western two-thirds of Dauphin Island, Alabama, 2015.

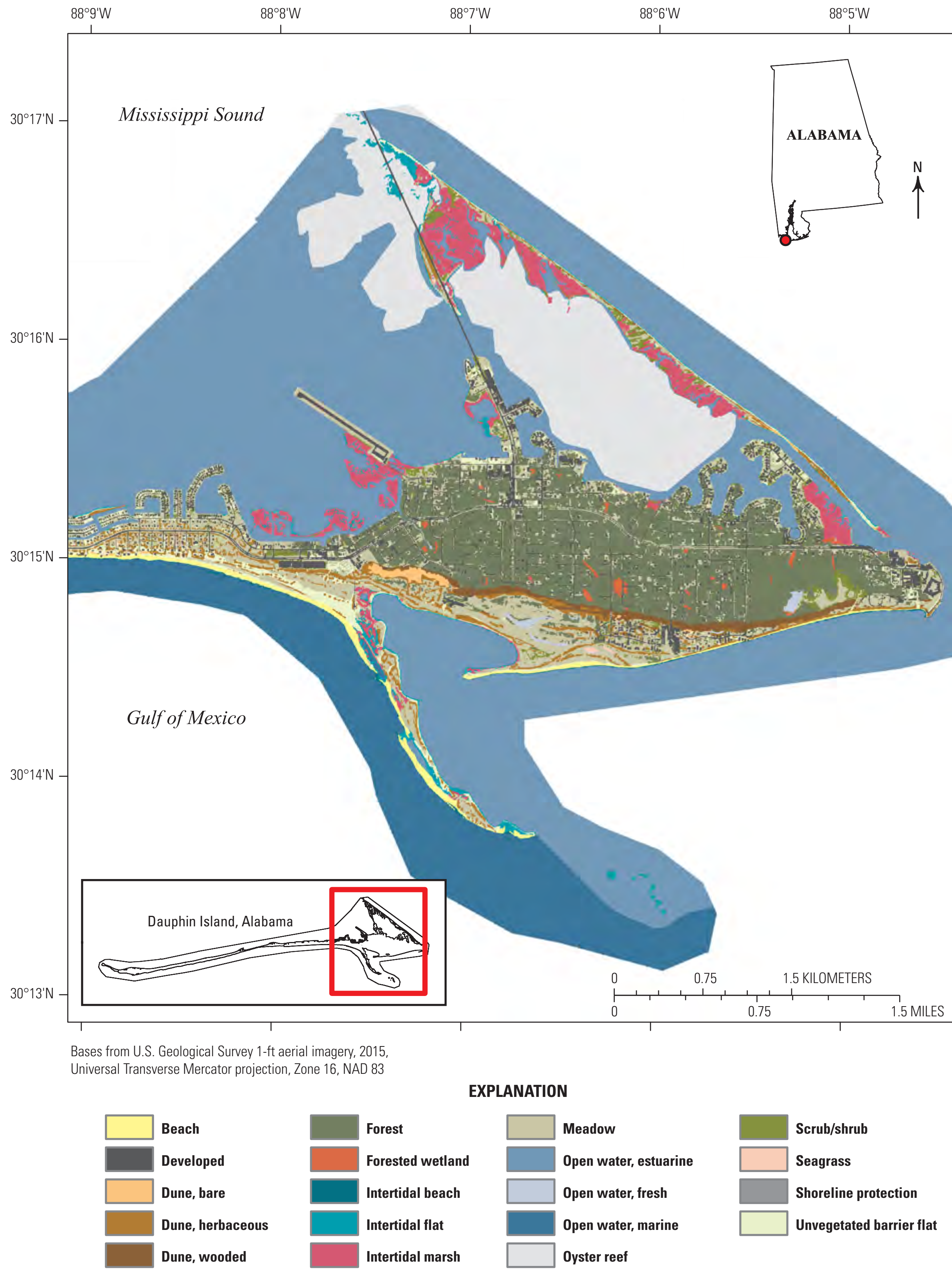

Figure 7. Habitat map for the eastern one-third of Dauphin Island, Alabama, 2015.

Table 4. Dominant vegetation and area mapped for each general habitat class, Dauphin Island, Alabama, 2015.

[—, not applicable]

Habitat	Dominant vegetation		Total area mapped, in square kilometers
Dune, bare	—		0.10
Dune, herbaceous	*Uniola paniculata, Schizachyrium maritimum, Quercus virginiana, Heterotheca subaxillaris*		1.09
Dune, wooded	*Ceratiola ericoides, Eragrostis secundiflora, Uniola paniculata, Chrysoma pauciflosculosa*		0.22
Meadow	*Spartina patens, Fimbristylis spadicea, Panicum repens, Hydrocotyle* spp.		3.60
Unvegetated barrier flat	*Spartina patens, Fimbristylis spadicea, Panicum repens, Hydrocotyle* spp.		1.05
Scrub/shrub	Canopy	*Pinus elliottii, Iva frutescens, Baccharis halimifolia, Ilex vomitoria*	0.47
	Ground	*Spartina patens, Iva frutescens, Panicum repens, Juncus roemerianus*	
Forest	Canopy	*Pinus elliottii, Quercus virginiana, Serenoa repens, Quercus nigra*	2.92
	Ground	*Serenoa repens, Smilax bona-nox, Ilex vomitoria, Osmundastrum cinnamomeum*	
Forested wetland	*Nyssa sylvatica*[1]		0.06
Intertidal beach	—		0.19
Beach	*Paspalum vaginatum*		0.84
Intertidal flat	*Distichlis spicata, Paspalum vaginatum*		0.55
Intertidal marsh	*Juncus roemerianus, Spartina alterniflora, Paspalum vaginatum, Fimbristylis spadicea*		1.22
Seagrass	*Halodule wrightii*[2]		0.95
Oyster reef	—		3.08
Shoreline protection	—		0.03
Developed	—		1.21
Open water, fresh	—		0.05
Open water, estuarine	—		24.46
Open water, marine	—		13.35

[1]Based on general observations in Audubon Bird Sanctuary; no actual data collected.

[2]Based on data collected by Barry Vittor and Associates, Inc., 2015.

Table 5. Error matrix for the Dauphin Island, Alabama, barrier island habitat map, 2015.

[DB, dune, bare; DH, dune, herbaceous; DW, dune, wooded; M, meadow; UBF, unvegetated barrier flat; SS, scrub/shrub; F, forest; IB, intertidal beach; B, beach; IF, intertidal flat; IM, intertidal marsh; %, percent. Bold numbers indicate instances where reference class matches habitat map class (that is, the count of sample locations that were mapped correctly)]

		Reference data (count per cell in matrix)													User's accuracy (%)
		DB	DH	DW	M	UBF	SS	F	IB	B	IF	IM	Other	Row total	
Map data	DB	**28**	2	1	0	0	0	0	0	0	0	0	0	31	90.32
	DH	1	**36**	4	4	1	0	0	0	0	0	0	0	46	78.26
	DW	0	4	**28**	2	0	1	7	0	0	0	0	0	42	66.67
	M	0	32	2	**113**	1	16	3	0	0	1	4	0	172	65.70
	UBF	0	3	0	4	**34**	1	0	0	0	4	0	0	46	73.91
	SS	0	0	0	8	0	**47**	2	0	0	0	2	0	59	79.66
	F	0	0	1	1	0	0	**73**	0	0	0	0	0	75	97.33
	IB	0	0	0	0	0	0	0	**26**	1	3	0	0	30	86.67
	B	1	1	0	0	0	0	0	3	**28**	3	0	0	36	77.78
	IF	0	0	0	3	4	0	0	0	1	**41**	2	0	51	80.39
	IM	0	0	0	36	0	4	2	0	0	1	**136**	0	179	75.98
	Other	0	0	0	2	0	0	0	1	0	13	1	**0**	17	–
	Column total	30	78	36	173	40	69	87	30	30	66	145	0	**784**	
Producer's accuracy (%)		93.33	46.15	77.78	65.32	85.00	68.12	83.91	86.67	93.33	62.12	93.79	–		
Overall accuracy (%): 75.26															
Kappa statistic: 0.72															

Conclusion

In this study, we produced a habitat map and conducted habitat-type, vegetation, and elevation surveys for Dauphin Island, Alabama. The habitat map provides a detailed high-resolution map that is specific to barrier island habitats, which was previously not available for Dauphin Island. The primary focus of the vegetation survey was to support the habitat map development through on-the-ground observations that could be used as validation points for the habitat map. The vegetation survey also provides useful information for characterizing the vegetation structure on Dauphin Island, and the elevation survey was used to help address elevation uncertainty issues for specific habitat zones. The habitat map and the vegetation survey will serve as baseline datasets for the ongoing Dauphin Island restoration feasibility study. In addition to tracking expected changes to the island due to restoration actions, these data provide detailed information for assessing and predicting change in response to gradual geomorphic processes and future episodic events.

References Cited

Acosta, A., Carranza, M.L., and Izzi, C.F., 2005, Combining land cover mapping of coastal dunes with vegetation analysis: Applied Vegetation Science, v. 8, p. 133–138.

Arundel, S.T., Archuleta, C.M., Phillips, L.A., Roche, B.L., and Constance, E.W., 2015, 1-meter digital elevation model specification: U.S. Geological Survey Techniques and Methods, book 11, chap. B7, 25 p. with appendixes, accessed April 3, 2017, at http://dx.doi.org/10.3133/tm11B7.

American Society for Photogrammetry & Remote Sensing [ASPRS], 2015, ASPRS positional accuracy standards for digital geospatial data: Photogrammetric Engineering & Remote Sensing, v. 81, p. A1–A26.

Barbier, E.B., Hacker, S.D., Kennedy, C., Koch, E.W., Stier, A.C., and Silliman, B.R., 2011, The value of estuarine and coastal ecosystem services: Ecological Monographs, v. 81, p. 169–193.

Blaschke, T., Hay, G.J., Kelly, M., Lang, S., Hofmann, P., Addink, E., Feitosa, R.Q., van der Meer, F., van der Werff, H., van Coillie, F., and Tiede, D., 2014, Geographic Object-Based Image Analysis—Towards a new paradigm: ISPRS Journal of Photogrammetry and Remote Sensing, v. 87, p. 180–191.

Boyer, T.P., Biddle, M., Habilton, M., Mishonov, A.V., Paver, C.R., Seidov, D., and Zweng, M., 2011, Gulf of Mexico Regional Climatology dataset: National Oceanic and Atmospheric Administration, National Centers for Environmental Information, accessed June 16, 2017, at http://dx.doi.org/10.7289/V5C53HSW.

Buffington, K.J., Dugger, B.D., Thorne, K.M., and Takekawa, J.Y., 2016, Statistical correction of lidar-derived digital elevation models with multispectral airborne imagery in tidal marshes: Remote Sensing of Environment, v. 186, p. 616–625.

Chust, G., Galparsoro, I., Borja, A., Franco, J., and Uriate, A., 2008, Coastal and estuarine habitat mapping, using LIDAR height and intensity and multi-spectral imagery: Estuarine, Coastal and Shelf Science, v. 78, p. 633–643.

Cohen, J., 1960, A coefficient of agreement for nominal scales: Educational and Psychological Measurement, v. 20, p. 37–46 accessed May 15, 2017, at https://dx.doi.org/10.1177/001316446002000104.

Cole, D.N., 1978, Estimating the susceptibility of wildland vegetation to trailside alteration: Journal of Applied Ecology, v. 15, p. 281–286.

Congalton, R.G., and Green, K., 2009, Assessing the accuracy of remotely sensed data principles and practices (2d ed.): Boca Raton, Fla., CRC Press, 183 p.

Cooper, H.M., and Chen, Q., 2013, Incorporating uncertainty of future sea-level rise estimates into vulnerability assessment: A case study in Kahului, Maui: Climatic Change, v. 121, p. 635–647.

Cowardin, L.M., Carter, V., Golet, F.C., and LaRoe, E.T., 1979, Classification of wetlands and deepwater habitats of the United States: Washington, D.C., U.S. Department of the Interior, Fish and Wildlife Service, Report FWS/OBS–79/31, 131 p.

Curtis, J.T., and McIntosh, R.P., 1951, An upland forest continuum in the prairie-forest border region of Wisconsin: Ecology, v. 32, p. 476–496.

De Reu, J., Bourgeois, J., Bats, M., Zwertvaegher, A., Gelorini, V., De Smedt, P., Chu, W., Antrop, M., De Maeyer, P., Finke, P., Van Meirvenne, M., Verniers, J., and Crombé, P., 2013, Application of the topographic position index to heterogeneous landscapes: Geomorphology, v. 186, p. 39–49.

Enwright, N.M., Borchert, S.M., Day, R.H., Feher, L.C., Osland, M.J., Wang, Lei, and Wang, Hongqing, 2017, Barrier island habitat map and vegetation survey, Dauphin Island, AL, 2015: U.S. Geological Survey data release, accessed June 22, 2017, at https://doi.org/10.5066/F7513WPC.

Fearnley, S., Brien, L., Martinez, L., Miner, M., Kulp, M., and Penland, S., 2009, Louisiana Barrier Island Comprehensive Monitoring Program (BICM), Volume 5: Chenier Plain, South-Central Louisiana, and Chandeleur Islands, Habitat mapping and change analysis 1996 to 2005, Part 1: Methods for habitat mapping and change analysis 1996 to 2005: New Orleans, University of New Orleans, Pontchartrain Institute for Environmental Sciences.

Finkbeiner, M., Stevenson, B., and Seaman R., 2001, Guidance for benthic habitat mapping: An aerial photographic approach: U.S. National Oceanic and Atmospheric Administration, Coastal Services Center, NOAA/CSC/20117-PUB.

Galbraith, H., DesRochers, D.W., Brown, S., and Reed, J.M., 2014, Predicting vulnerabilities of North American shorebirds to climate change: PLoS ONE, v. e108899.

Gibson, D.J., and Looney, P.B., 1992, Seasonal variation in vegetation classification on Perdido Key, a barrier island off the coast of the Florida panhandle: Journal of Coastal Research, v. 8, p. 943–956.

Heidemann, H.K., 2014, Lidar base specification (ver. 1.2, November 2014): U.S. Geological Survey Techniques and Methods, book 11, chap. B4, 67 p. with appendixes, accessed April 3, 2017, at https://dx.doi.org/10.3133/tm11B4.

Homer, C.G., Dewitz, J.A., Yang, L., Jin, S., Danielson, P., Xian, G., Coulston, J., Herold, N.D., Wickham, J.D., and Megown, K., 2015, Completion of the 2011 National Land Cover Database for the conterminous United States—Representing a decade of land cover change information: Photogrammetric Engineering and Remote Sensing, v. 81, p. 345–354.

Hudak, A.T., Evans, J.S., and Smith, A.M.S., 2009, LiDAR utility for natural resource managers: Remote Sensing, v. 1, p. 934–951.

Hunter, G.J., and Goodchild, M.F., 1995, Dealing with error in spatial databases: A simple case study: Photogrammetric Engineering & Remote Sensing, v. 61, p. 529–537.

Katselidis, K.A., Schofield, G., Stamou, G., Dimopoulos, P., and Pantis J.D., 2014, Employing sea-level rise scenarios to strategically select sea turtle nesting habitat important for long-term management at a temperate breeding area: Journal of Experimental Marine Biology and Ecology, v. 450, p. 47–54.

Kindinger, J.L., Buster, N.A., Flocks, J.G., Bernier, J.C., and Kulp, M.A., 2013, Louisiana Barrier Island Comprehensive Monitoring (BICM) program summary report: Data and analyses 2006 through 2010: U.S. Geological Survey Open-File Report 2013–1083, 86 p., accessed April 3, 2017, at http://pubs.usgs.gov/of/2013/1083/.

Lea, Chris, and Curtis, A.C., 2010, Thematic accuracy assessment procedures, National Park Service Vegetation Inventory, version 2.0: National Park Service, Natural Resource Report NPS/2010/NRR—2010/204, 116 p.

Leatherman, S.P., 1979, Barrier Island Handbook: Amherst, Mass., National Park Service, 101 p.

Lester, L.A., Ramierez, M.G., Kneidel, A.H., and Heckscher, C.M., 2016, Use of a Florida gulf coast barrier island by spring trans-gulf migrants and the projected effects of sea level rise on habitat availability: PLoS ONE, v. e0148975, accessed March 13, 2017, at https://doi.org/10.1371/journal.pone.0148975.

Lucas, K.L., and Carter, G.A., 2010, Decadal changes in habitat-type coverage on Horn Island, Mississippi, U.S.A.: Journal of Coastal Research, v. 26, p. 1142–1148.

May, E.B., 1971, A survey of the oyster and oyster shell resources in Alabama: Alabama Marine Resources Bulletin, v. 4, p. 1–53.

McCarthy, M.J., and Halls, J.N., 2014, Habitat mapping and change assessment of coastal environments: An examination of WorldView-2, QuickBird, and IKONOS satellite imagery and airborne LiDAR for mapping barrier island habitats: ISPRS International Journal of Geo-Information, v. 3, p. 297–325.

Medeiros, S., Hagen, S., Weishampel, J., and Angelo J., 2015, Adjusting lidar-derived digital terrain models in coastal marshes based on estimated aboveground biomass density: Remote Sensing, v. 7, p. 3507–3525.

Meng, X., Wang, L., and Currit, N., 2009, Morphology-based building detection from airborne lidar data: Photogrammetric Engineering & Remote Sensing, v. 75, p. 437–442.

Morton, R.A., 2008, Historical changes in the Mississippi-Alabama barrier-island chain and the roles of extreme storms, sea level, and human activities: Journal of Coastal Research, v. 24, p. 1587–1600.

Myint, S.W., Gober, P., Brazel, A., Grossman-Clarke, S., and Weng, Q., 2006, Per-pixel vs. object-based classification of urban land cover extraction using high spatial resolution imagery: Remote Sensing of Environment, v. 115, p. 1145–1161.

National Oceanic and Atmospheric Administration [2013], Extreme Water Levels 8735180 Dauphin Island, AL webpage, assessed October 10, 2016, at https://tidesandcurrents.noaa.gov/est/est_station.shtml?stnid=8735180.

Oertel, G.F., 1985, The barrier island system: Marine Geology, v. 63, p. 1–18.

Otvos, E.G.J., 1970, Development and migration of barrier islands, northern Gulf of Mexico: Geological Society of America Bulletin, v. 81, p. 241–246.

Otvos, E.G.J., and Carter, G.A., 2008, Hurricane degradation—Barrier development cycles, northeastern Gulf of Mexico: Landform evolution and island chain history: Journal of Coastal Research, v. 24, p. 463–478.

Pilkey, O.H., and Cooper, J.A.G., 2014, The last beach: Durham, North Carolina, Duke University Press Books, 256 p.

Poulter, B., and Halpin, P.N., 2008, Raster modelling of coastal flooding from sea-level rise: International Journal of Geographical Information Science, v. 22, no. 2, p. 167–182, accessed October 10, 2016, at https://dx.doi.org/10.1080/13658810701371858.

Stutz, M.L., and Pilkey, O.H., 2011, Open-ocean barrier islands: Global influence of climatic, oceanographic, and depositional settings: Journal of Coastal Research, v. 27, p. 207–222.

Sugarbaker, L.J., Constance, E.W., Heidemann, H.K., Jason, A.L., Lukas, V., Saghy, D.L., and Stoker, J.M., 2014, The 3D Elevation Program initiative—A call for action: U.S. Geological Survey Circular 1399, 35 p., accessed April 3, 2017, at https://dx.doi.org/10.3133/cir1399.

Trimble, 2016, Trimble eCognition Developer version 9.2 user guide: Munich, Germany, Trimble Germany GmbH, 265 p.

U.S. Department of Agriculture, 2013, NAIP imagery, accessed September 9, 2015, at https://www.fsa.usda.gov/programs-and-services/aerial-photography/imagery-programs/naip-imagery/.

Weiss, A.D., 2001, Topographic position and landforms analysis: ESRI Users Conference, San Diego, Calif., accessed September 19, 2016, at http://www.jennessent.com/downloads/tpi-poster-tnc_18x22.pdf.

Wernette, P., Houser, C., and Bishop, M.P., 2016, An automated approach for extracting Barrier Island morphology from digital elevation models: Geomorphology, v. 262, p. 1–7.

Wechsler, S.P., and Kroll, C.N., 2006, Quantifying DEM uncertainty and its effect on topographic parameters: Photogrammetric Engineering & Remote Sensing, v. 72, p. 1081–1090.

Zervas, C., 2013, Extreme water levels of the United States 1893–2010: National Oceanic and Atmospheric Administration, NOAA Technical Report NOS CO-OPS 067, 200 p.

Zinnert, J.C., Shiflett, S.A., Via, S., Bissett, S., Dows, B., Manley, P., and Young, D.R., 2016, Spatial–temporal dynamics in barrier island upland vegetation: The overlooked coastal landscape: Ecosystems, v. 19, p. 685–697.

Publishing support provided by
Lafayette Publishing Service Center

Enwright and others—**Barrier Island Habitat Map and Vegetation Survey—Dauphin Island, Alabama, 2015**—Open-File Report 2017–1083

ISSN 2331-1258 (online)
https://doi.org/10.3133/ofr20171083